Highly Selective Luminescent Sensing of Fluoride and Organic Small-Molecule Pollutants Based on Novel Lanthanide Metal-Organic Frameworks

ARTICLE *in* INORGANIC CHEMISTRY · JULY 2013

Impact Factor: 4.76 · DOI: 10.1021/ic400770j · Source: PubMed

4 AUTHORS, INCLUDING:

Wei Shi
Nankai University
153 PUBLICATIONS **6,245** CITATIONS

SEE PROFILE

Inorganic Chemistry

Article

pubs.acs.org/IC

Highly Selective Luminescent Sensing of Fluoride and Organic Small-Molecule Pollutants Based on Novel Lanthanide Metal−Organic Frameworks

Jing-Min Zhou, Wei Shi,* Na Xu, and Peng Cheng*

Department of Chemistry, Key Laboratory of Advanced Energy Materials Chemistry (MOE), Nankai University, Tianjin 300071, People's Republic of China

Supporting Information

ABSTRACT: Two novel isostructural lanthanide metal−organic frameworks (Ln-MOFs), $[Ln_2(BPDC)(BDC)_2(H_2O)_2]_n$ (Ln = Eu (**1**) and Tb (**2**)), have been successfully synthesized via a mixed ligand approach using 2,2′-bipyridine-3,3′-dicarboxylic acid (H_2BPDC) and 1,4-benzenedicarboxylic acid (H_2BDC) under hydrothermal conditions. Structural analysis shows that two lanthanide ions are 4-fold linked by two κ^1-κ^1-μ_2 carboxylates from BDC^{2-} and the other two κ^2-κ^1-μ_2 carboxylates from $BPDC^{2-}$ to form a binuclear core. The binuclear units are further connected by BDC^{2-} and $BPDC^{2-}$ to build a three-dimensional framework possessing **tfz-d** topology with the short (Schläfli) vertex symbol $\{4^3\}_2\{4^6\cdot6^{18}\cdot8^4\}$. Moreover, isostructural doped Ln-MOFs $[Eu_{2x}Tb_{2(1-x)}(BPDC)(BDC)_2(H_2O)_2]_n$ (x = 0.1 (**1a**), 0.3 (**1b**), 0.5 (**1c**), 0.7 (**1d**), and 0.9 (**1e**)) were also successfully synthesized. Thermal gravimetric analyses (TGA) reveal high thermal stability of these Ln-MOFs. Luminescent measurements indicate that the characteristic sharp emission bands of Eu^{3+} and Tb^{3+} ions are simultaneously observed in **1a**−**e**. Further luminescent studies reveal that **1**, **2**, and **1a** not only display a high-sensitivity sensing function with respect to fluoride but also exhibit significant solvent-dependent luminescent response to small-molecule pollutants, such as formaldehyde, acetonitrile, and acetone.

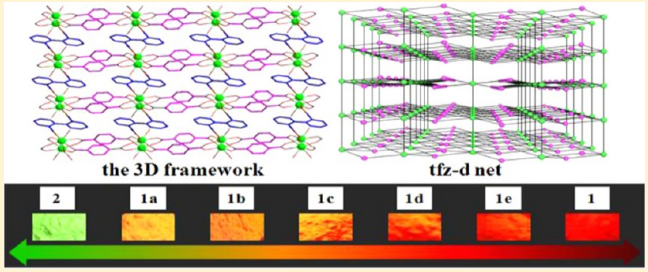

INTRODUCTION

In recent years, the design and construction of lanthanide metal−organic frameworks (Ln-MOFs) have been extensively concerned because of their intriguing topological structures, as well as the interesting photoluminescence resulting from the 4f electronic shell.[1−3] Increasing interest was found in the recognition and sensing of inorganic ions and small organic molecules using Ln-MOFs as luminescent sensors for their important roles in biological and environmental systems.[4] Ln-MOFs can be considered as promising luminescent sensing materials because their inorganic and organic components can provide platforms to generate visible luminescence when induced by UV light. Many lanthanide compounds are well-known for their intense photoluminescence arising from f−f or f−d energy transfer tuned by suitable adjacent chromophores, such as phenyl and pyridyl, which can be called the "antenna".[5]

Among the lanthanide ions, Eu^{3+} and Tb^{3+} could show intense red and green emission, respectively. Multiple emission colors usually can be achieved by adjusting the relative amounts of red and green components in singular Ln-based compound.[6] Materials emitting multiple colors under single-wavelength excitation are of significant importance in the field of light display, lasers, and optoelectronic devices. With regards to tunable emission colors based on the different lanthanide ions, some very-well characterized f−f hybrid compounds have been documented.[7] Indeed, molecular f−f hybrid complexes could be rationally synthesized via clever ligand design apporach.[8,9] However, color modulation in Ln-MOFs by varying the doping concentration is yet to be properly explored.

In this context, Eu^{3+} and Tb^{3+} could be one of the best candidates as luminescent centers. It is also important to find appropriate ligand to act as antenna to effectively transfer the energy to the luminescent centers. In view of our previous work,[10] aromatic-carboxylic groups are good luminescent chromophores. Therefore, we introduce aromatic-carboxylic acid containing phenyl and pyridyl groups as ligands, which have been proven to show a strong antenna effect. In this contribution, two Ln-MOFs, namely $[Ln_2(BPDC)(BDC)_2(H_2O)_2]_n$ (Ln = Eu (**1**); Tb (**2**); H_2BPDC = 2,2′-bipyridine-3,3′-dicarboxylic acid; H_2BDC = 1,4-benzenedicarboxylic acid), as well as a series of doped Ln-MOFs $[Eu_{2x}Tb_{2(1-x)}(BPDC)(BDC)_2(H_2O)_2]_n$ (x = 0.1 (**1a**), 0.3 (**1b**), 0.5 (**1c**), 0.7 (**1d**), and 0.9 (**1e**)) have been synthesized via a mixed ligand approach under hydrothermal conditions. Ln-MOFs **1**, **2**, and **1a** display a high-sensitivity sensing function with respect to fluoride and small-molecule organic solvent pollutants, particularly formaldehyde, acetonitrile, and acetone.

Received: March 28, 2013
Published: July 2, 2013

EXPERIMENTAL SECTION

Materials and Methods. H_2BPDC and $Ln(OH)_3$ were prepared by the literature method,[11] and the other chemicals purchased were of reagent grade and used without further purification. Analyses for C, H, and N were carried out on a Perkin-Elmer 240 CHN elemental analyzer. IR was recorded in the range 400−4000 cm^{-1} on a Bruker TENOR 27 spectrophotometer using KBr pellets. Powder X-ray diffraction measurements were recorded on a Rigaku D/Max-2500 X-ray diffractometer using Cu Kα radiation. TGA were performed on a Labsys NETZSCH TG 209 Setaram apparatus with a heating rate of 10 °C/min in nitrogen atmosphere. The fluorescent spectra were measured on a Varian Cary Eclipse Fluorescence spectrophotometer. The luminescent properties were investigated in the solid state and in suspensions at room temperature. The suspensions were prepared by introducing each sample (3.0 mg) as a powder into different solvents (each 2.0 mL) and were then vigorously agitated using ultrasound. The photoluminescent (PL) spectra of the suspensions were measured after aging overnight.

X-ray Crystallography. Diffraction intensity data for single crystals of **1** and **2** were collected on a Agilent Technologies SuperNova Single Crystal Diffractometer at 293(2) K equipped with graphite-monochromatic Mo Kα radiation (λ = 0.71073 Å). The structures were solved by SHELXS (direct methods) and refined by SHELXL (full matrix least-squares techniques) in the Olex2 package.[12] The selected crystal parameters, data collection, and refinements are summarized in Table 1.

Table 1. Crystal Data and Structural Refinement Parameters for 1 and 2

	1	2
formula	$C_{14}H_9EuNO_7$	$C_{14}H_9TbNO_7$
fw	455.18	462.15
λ/Å	0.71073	0.71073
crystal system	monoclinic	monoclinic
space group	*C*2/*c*	*C*2/*c*
a (Å)	24.89	24.80
b (Å)	9.18	9.12
c (Å)	14.52	14.52
α (deg)	90	90
β (deg)	124.31	124.31
γ(deg)	90	90
V/Å^3	2740.3(5)	2712.4(5)
Z	8	8
ρ_{calc} /mg mm^{-3}	2.207	2.263
μ/mm^{-1}	4.617	5.254
reflns collected/unique	8457/2407	4753/2388
R(int)	0.0366	0.0306
2θ range/deg	6.54−50.02	6.56−50.02
F(000)	1752.0	1768.0
GOF on F^2	1.045	1.128
$R_1/wR_2[I > 2\sigma(I)]$	R_1 = 0.0194, wR_2 = 0.0466	R_1 = 0.0228, wR_2 = 0.0577
R_1/wR_2 (all data)	R_1 = 0.0208, wR_2 = 0.0475	R_1 = 0.0238, wR_2 = 0.0582
largest diff. peak/hole/e Å^{-3}	0.47/−0.55	0.56/−1.53

Synthesis of $[Ln_2(BPDC)(BDC)_2(H_2O)_2]_n$ (1 and 2). A mixture of $Ln(OH)_3$ (0.4 mmol, Ln = Eu (**1**), Tb (**2**)), H_2BPDC (0.6 mmol, 0.1466 g), H_2BDC (0.3 mmol, 0.0499 g), and H_2O (10 mL) was added in a 25 mL Teflon-lined stainless steel reactor and heated at 160 °C for 72 h and, then, slowly cooled to room temperature. Block-shaped single crystals suitable for X-ray data collection were obtained by filtration, washed with distilled water, and air-dried. Yield: 28% and 30% based on H_2BDC for **1** and **2**, respectively. Elemental analysis found (calcd) for $Eu_2C_{28}N_2O_{14}H_{18}$ (**1**): C, 37.21 (36.94); H, 2.10 (1.99); N, 3.13 (3.08). IR bands (KBr, ν/cm^{-1}) for **1**: 3486(br), 1558(vs), 1399(s), 1161(m), 1020(m), 873(m), 817(m), 753(s), 509(s), 442(m). Elemental analysis found (calcd) for $Tb_2C_{28}N_2O_{14}H_{18}$ (**2**): C, 35.99 (36.38); H, 2.09 (1.96); N, 2.86 (3.03). IR bands (KBr, ν/cm^{-1}) for **2**: 3481(br), 1581(vs), 1400(s), 1162(m), 1020(m), 876(m), 818(m), 753(s), 509(s), 443(m).

Synthesis of $[Eu_{2x}Tb_{2(1-x)}(BPDC)(BDC)_2(H_2O)_2]_n$ (1a−e). The synthesis of doped Ln-MOFs **1a−e** were performed following a similar procedure of **1** as described above, in which mixed $Eu(OH)_3$ (0.4*x* mmol) and $Tb(OH)_3$ (0.4(1 − *x*) mmol) (*x* = 0.1 (**1a**), 0.3 (**1b**), 0.5 (**1c**), 0.7 (**1d**), and 0.9 (**1e**)) took the place of pure $Eu(OH)_3$. Block-shaped single crystals were obtained by filtration, washed with distilled water, and air-dried. Yield: 41%, 38%, 33%, 31%, and 30% based on H_2BDC for **1a−e**, respectively.

The chemical composition of the doped Ln-MOFs **1a−e** was determined by inductively coupled plasma (ICP) (Supporting Information Table S1) and elemental analysis (EA). As shown in Supporting Information Figure S1, the FTIR spectra of these doped Ln-MOFs are similar to the pure Ln-MOFs **1** and **2** indicating the doped ones are isostructural to Ln-MOFs **1** and **2**, which are further confirmed by PXRD measurements (see below).

Elemental analysis found (calcd) for $Eu_{0.23}Tb_{1.77}C_{28}N_2O_{14}H_{18}$ (**1a**): C, 36.69 (36.44); H, 2.08 (1.97); N, 3.12 (3.04). $Eu_{0.56}Tb_{1.44}C_{28}N_2O_{14}H_{18}$ (**1b**): C, 36.80 (36.54); H, 2.31 (1.97); N, 3.32 (3.04). $Eu_{0.96}Tb_{1.04}C_{28}N_2O_{14}H_{18}$ (**1c**): C, 36.80 (36.65); H, 2.32 (1.98); N, 3.14 (3.05). $Eu_{1.34}Tb_{0.66}C_{28}N_2O_{14}H_{18}$ (**1d**): C, 36.51 (36.76); H, 2.28 (1.98); N, 3.06 (3.06). $Eu_{1.76}Tb_{0.24}C_{28}N_2O_{14}H_{18}$ (**1e**): C, 36.93 (36.87); H, 2.44 (1.99); N, 3.08 (3.07).

RESULTS AND DISCUSSION

Crystal Structure. Single-crystal X-ray crystallography determinations reveal that Ln-MOFs **1** and **2** are isostructurally crystallized in monoclinic space group of *C*2/*c*. The structure of **1** is described here representatively. As shown in Figure 1, Ln-MOF **1** consists of one crystallographically independent eight-coordinated Eu^{3+} ion, one BDC^{2-} anion, half of a $BPDC^{2-}$ anion, and one H_2O molecule per asymmetric unit. The Eu−O bond lengths vary from 2.286(2) to 2.589(2) Å (average 2.413 Å). Eight-coordinate geometries are usually taken as the D_{2d} dodecahedron (DD), C_{2v} bicapped trigonal prism (TP), and D_{4d} square antiprism (SAP). The semiquantitative method of polytopal analysis is performed to further evaluate the polyhedral shape of the metal coordination sphere. The smallest shape values with SAP ensure D_{4d} site symmetry (Supporting Information Table S2).[13] Therefore, the coordination geometry of Eu^{3+} ion can be viewed as a slightly distorted square antiprism, with the basal planes made by atoms of O4B, O5A, O6, and O7 and O1A, O2, O3A, and O6A. Two oxygen atoms from carboxyl groups of $BPDC^{2-}$ bridge two Eu^{3+} ion, thus forming an edge-sharing binuclear unit with Eu···Eu distance of 3.963(1) Å. In the unit, there are two different kinds of bridging modes for four carboxyl groups: two from BDC^{2-} in bidentate (κ^1-κ^1-μ_2) mode and the other two from $BPDC^{2-}$ in tridentate (κ^2-κ^1-μ_2) mode (Scheme 1). Adjacent binuclear units are connected by κ^1-κ^1-μ_2 carboxyl groups of BDC^{2-} to generate one-dimensional chain structure (Figure 2a) and further form an infinite layer through the linkers (κ^1-κ^2)-(κ^1-κ^2)-μ_4-$BPDC^{2-}$ (Figure 2b) or (κ^1-κ^1)-(κ^1-κ^1)-μ_4-BDC^{2-} (Figure 2c). Then the layers are connected by the linkers from the third direction into a three-dimensional (3D) network (Figure 2d). The 3D framework shows one-dimensional (1D) channels with a transverse section of ~2.8 × 3.0 Å^2 along the [0, 0, 1] direction (Supporting Information Figure S2). There are hydrogen bonds (O−H···O = 2.8310(2) and O−H···N = 2.7986(2) Å) in the structure (Supporting

dx.doi.org/10.1021/ic400770j | Inorg. Chem. 2013, 52, 8082−8090

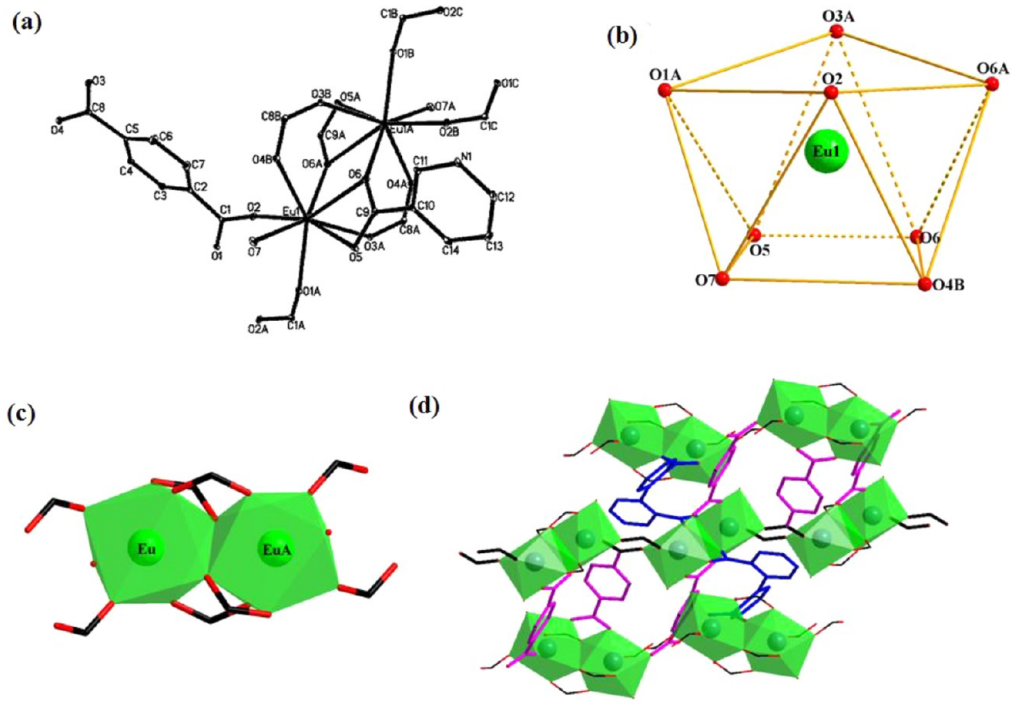

Figure 1. Crystal structure of **1**: (a) ORTEP drawing of the structural unit (thermal ellipsoids are drawn at the 30% probability level; H atoms were omitted for clarity), (b) the coordination geometries of Eu^{3+} ions, (c) the connection mode of Eu^{3+} ions in a binuclear unit, (d) linkages between binuclear units. Eu: green, O: red, N: blue, and C: black.

Scheme 1. Coordination Modes of the Ligands

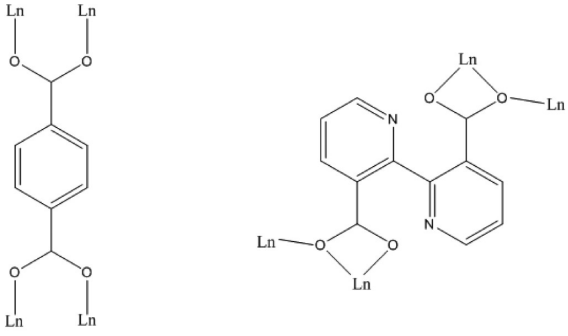

κ^1- κ^1-μ_2- carboxyl group
$(\kappa^1$-$\kappa^1)$-$(\kappa^1$-$\kappa^1)$-μ_4-BDC^{2-}

κ^2- κ^1-μ_2- carboxyl group
$(\kappa^1$-$\kappa^2)$-$(\kappa^1$-$\kappa^2)$-μ_4-$BPDC^{2-}$

Information Figure S3), which may enhance the stability of the structure.

In order to simplify the complicated framework, the network topology has been analyzed by the freely available computer program TOPOS.[14] If each Ln_2 binuclear unit is considered as an eight-connected node which links with six BDC^{2-} anions and two $BPDC^{2-}$ anions,[15] $BPDC^{2-}$ anions serve as bridging linkers, and BDC^{2-} anions are three-connected nodes which link Ln_2 binuclear units, the structure can be considered as a 3,8-connected net named **tfz-d** (Figure 3). This topology is also known in MOF chemistry, and the point symbol of the topology can be expressed as $\{4^3\}_2\{4^6{\cdot}6^{18}{\cdot}8^4\}$.[16] Such a kind of net is rarely reported in pure Ln-MOFs.

Powder X-ray Diffraction. To confirm the phase purity of **1**, **2**, and **1a**−**e**, the powder X-ray diffraction (PXRD) patterns have been carried out at room temperature. As shown in Supporting Information Figure S4a, the diffraction peaks of the as-synthesized samples are almost in agreement with the simulated data, confirming the phase purity of the compounds. It is also clear that the structures of the doped Ln-MOFs **1a**−**e** are isostructural to pure Ln-MOFs **1** and **2**. A heated sample of this Ln-MOF can be obtained when heated at 200 °C for 12 h. The experimental PXRD pattern of the activated sample is almost identical to the simulated one (Figure S4b), illustrating that the basic framework is retained.

Thermal Gravimetric Analyses. Thermal gravimetric analyses (TGA) of **1** and **2** were performed in the temperature range of 30−900 °C (Supporting Information Figure S5). The trends of weight loss are similar due to the isostructural nature. Both of them almost do not lose any obvious weight until 200 °C, suggesting no guest molecules in the lattice, as confirmed by the single crystal X-ray diffraction analysis. Because of the hydrogen-bonding interaction and the steric hindrance, the coordinated water molecules are difficult to remove at low temperature. As can be seen from Supporting Information Figure S5, about half of the coordinated water molecules leave at 260 °C and all of them leave until 370 °C. Subsequently, the frameworks begin to decompose. In general, these compounds have a certain thermal stability, which can be verified by the FTIR spectrum and PXRD at different temperatures (Supporting Information Figures S1 and S4).

Luminescent Properties. The solid-state emission spectra of **1**, **2**, and **1a**−**e** at room temperature are shown in Figure 4. When excited at 300 nm, Ln-MOF **1** exhibits four characteristic transitions of Eu^{3+} ion: 594, 614, 652, and 700 nm, ascribed to $^5D_0 \rightarrow {}^7F_J$ (J = 1−4),[17] respectively. The strongest $^5D_0 \rightarrow {}^7F_2$ transition is an electric dipole transition, the so-called hypersensitive transition, and is responsible for the brilliant-red emission. Although the magnetic dipole transition of $^5D_0 \rightarrow {}^7F_1$, which is fairly insensitive to the coordination environment of the Eu^{3+} ion, is also present, it is clearly less intense than the

dx.doi.org/10.1021/ic400770j | Inorg. Chem. 2013, 52, 8082−8090

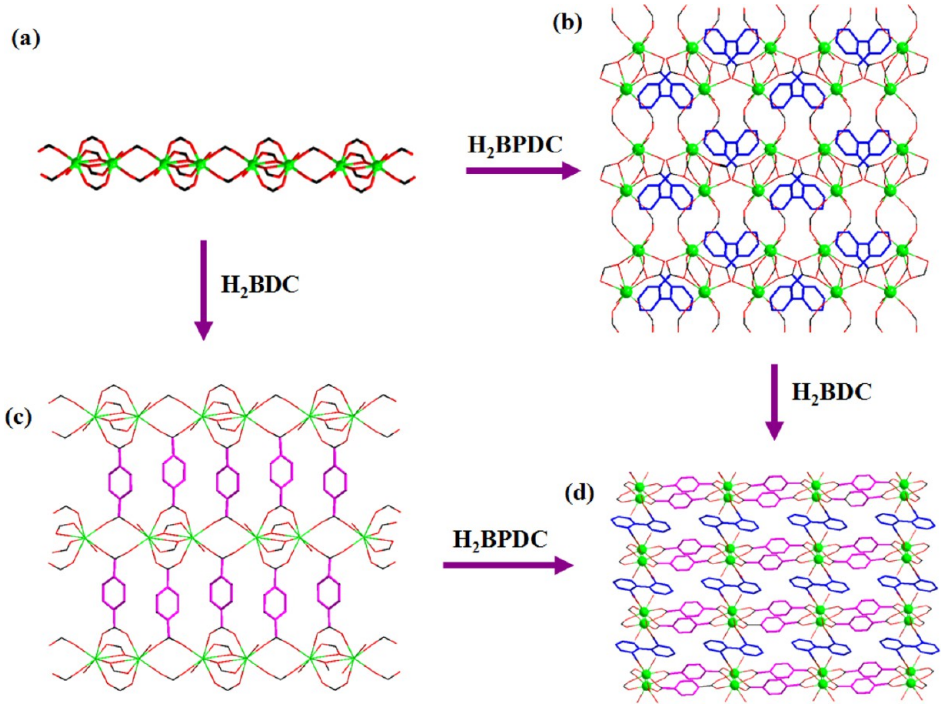

Figure 2. Structure of Ln-MOF **1**: (a) the Ln chain obtained from binuclear units linked by carboxyl groups; (b) the 2D plane along the direction [1, 0, 0] through the linker H_2BPDC (blue); (c) the 2D plane along the direction [0, 0, 1] through the linker H_2BDC (pink); (d) the 3D framework along the direction [0, 0, 1].

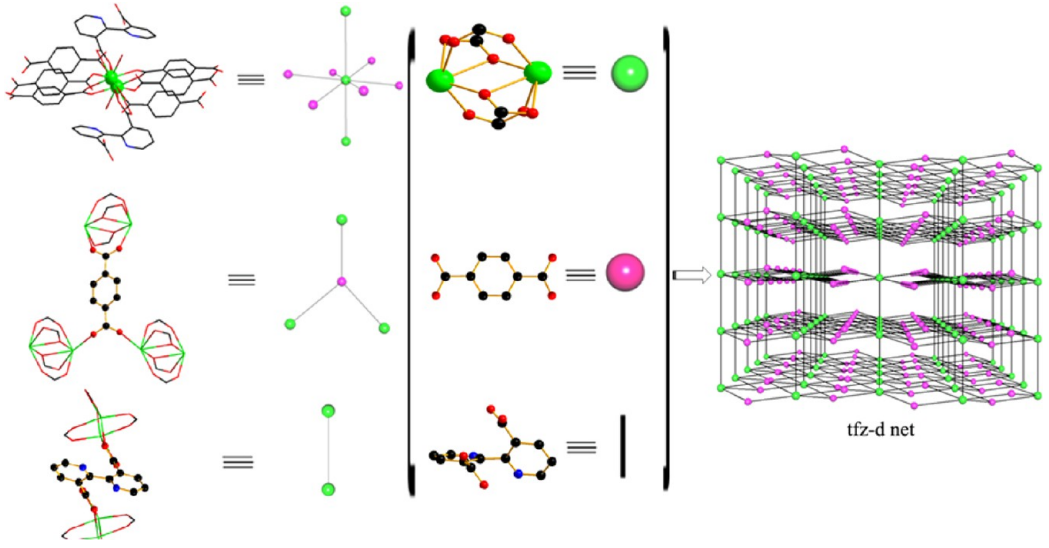

Figure 3. Simplified topological structure: (green) Ln_2 binuclear units; (pink) BDC^{2-} anions.

$^5D_0 \rightarrow {}^7F_2$ transition. The above results suggest the absence of inversion symmetry of Eu^{3+} sites in Ln-MOF **1**, which is in agreement with the single-crystal X-ray analysis. Ln-MOF **2** yields hypersensitive green luminescence when excited at 300 nm. The distinct emissions at 487, 544, 585, and 621 nm are assigned to the transitions of $^5D_4 \rightarrow {}^7F_J$ (J = 6–3) of the Tb^{3+} ion, respectively,[17–19] and the color is dominated by the emission of $^5D_4 \rightarrow {}^7F_5$ at 544 nm.

When the doped samples of **1a–e** are excited at 300 nm, the characteristic sharp emission bands of Eu^{3+} and Tb^{3+} ions simultaneously exist (Figure 4**a**). The emission intensity of Eu^{3+} and Tb^{3+} are closely related with the proportion. Since the content of Eu^{3+} in **1a–e** is increased, the characteristic emission intensity of Eu^{3+} gradually increases while the characteristic emission intensity of Tb^{3+} decreases step by step. The doped **1a–e** illuminated with 254 nm laboratory UV light at room temperature display bimodal luminescence and the Eu^{3+}/Tb^{3+} percentage-tuned intermediate colors (Figure 4**b**). There is almost no ligand-base emission in the photoluminescent spectra of these Ln-MOFs (Supporting Information Figure S6), illustrating that the energy transfer from the ligands $BPDC^{2-}$ or BDC^{2-} to the lanthanide center is very effective and can sensitize the luminescence of Eu^{3+} and Tb^{3+} ions by UV radiation to a large extent.[18b,c]

In order to investigate anion recognition of the Ln-MOFs, the suspension-state luminescent experiments are performed.

dx.doi.org/10.1021/ic400770j | Inorg. Chem. 2013, 52, 8082–8090

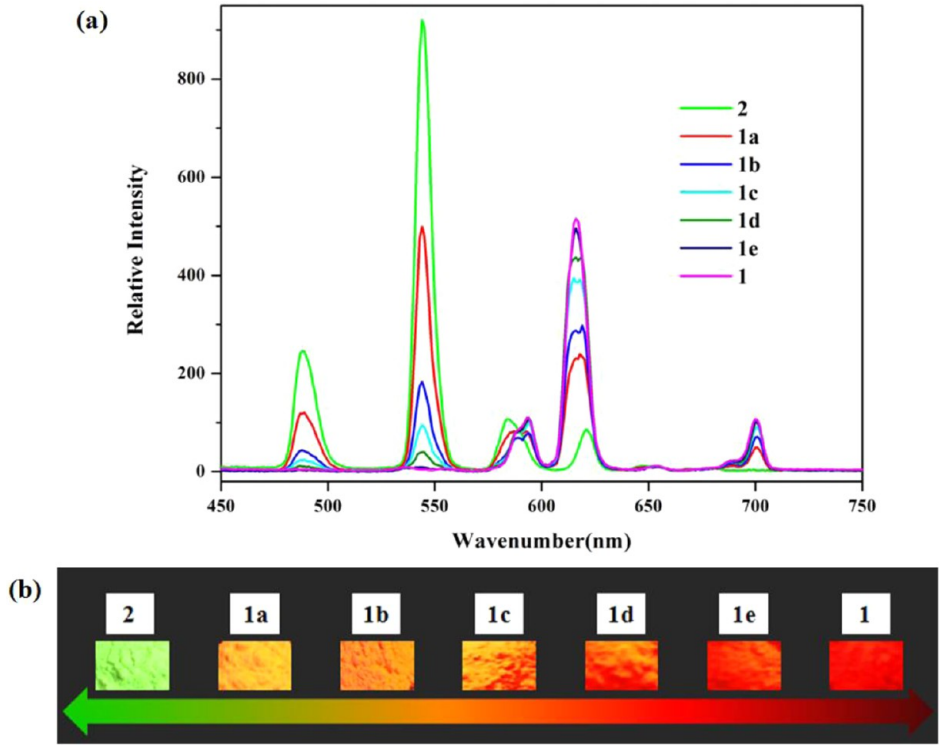

Figure 4. (a) Solid-state PL spectra of **1**, **2**, and **1a**−**e** at room temperature (excited at 300 nm). (b) Samples of **1**, **2**, and **1a**−**e** illuminated with 254 nm laboratory UV light at room temperature.

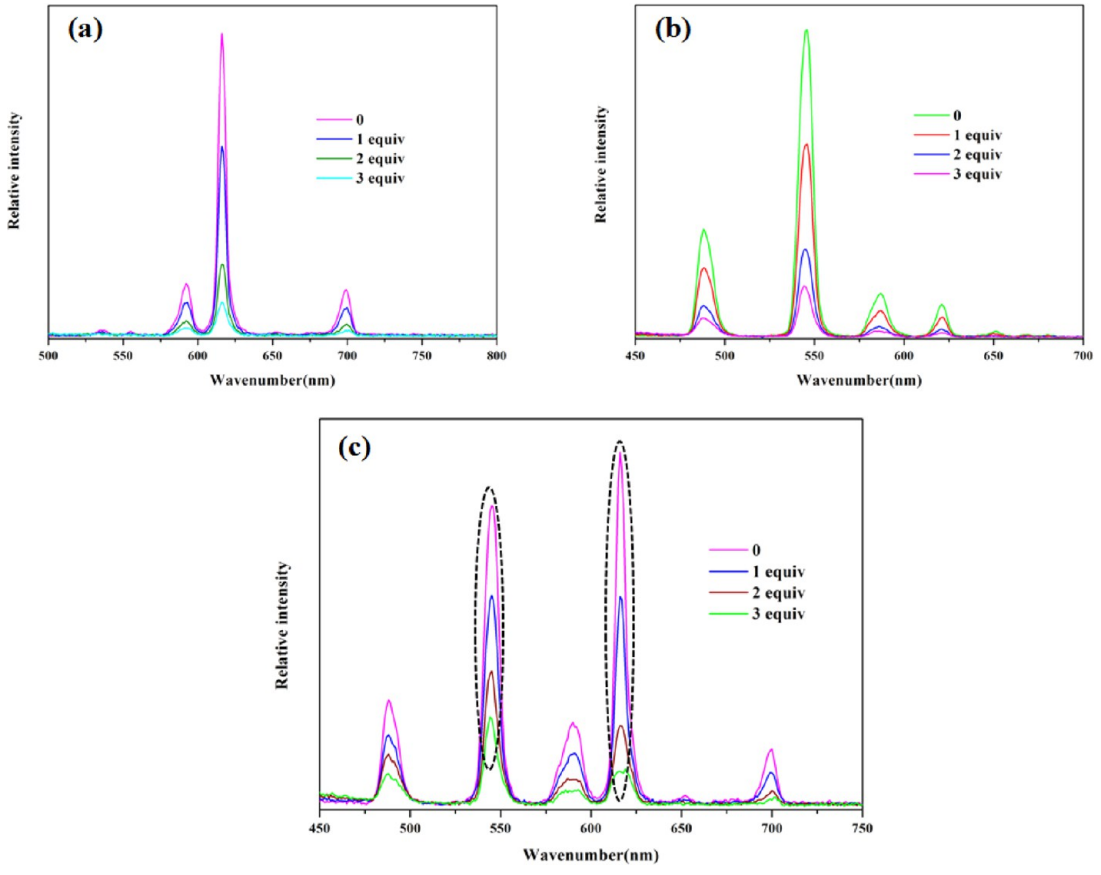

Figure 5. Emission spectra of **1** (a), **2** (b), and **1a** (c) dispersed in H_2O at room temperature in the presence of 0−3 equiv of F^- ions (The blank experiment results are shown in Supporting Information Figures S11−S13).

dx.doi.org/10.1021/ic400770j | *Inorg. Chem.* 2013, 52, 8082−8090

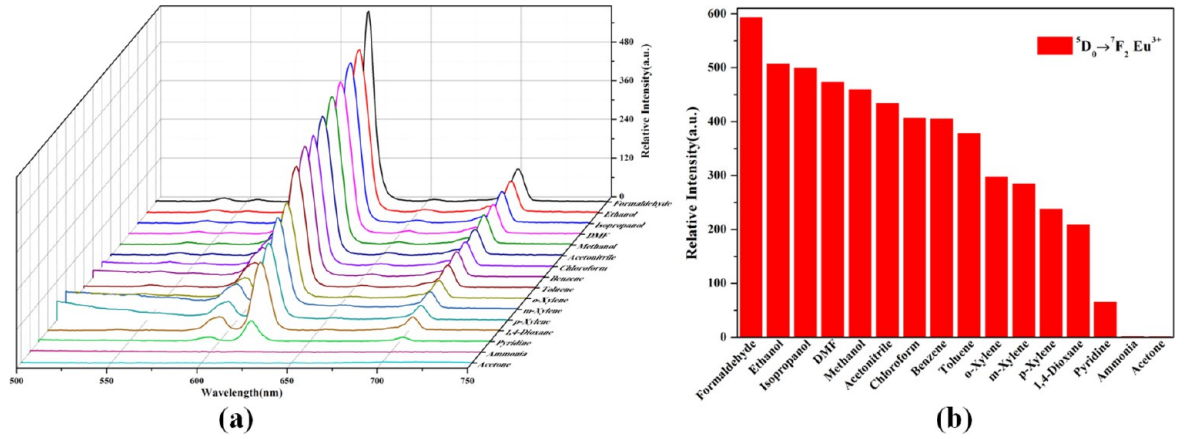

Figure 6. (a) PL spectra and (b) the $^5D_0 \rightarrow {}^7F_2$ transition intensities of **1** dispersed into different solvents when excited at 300 nm.

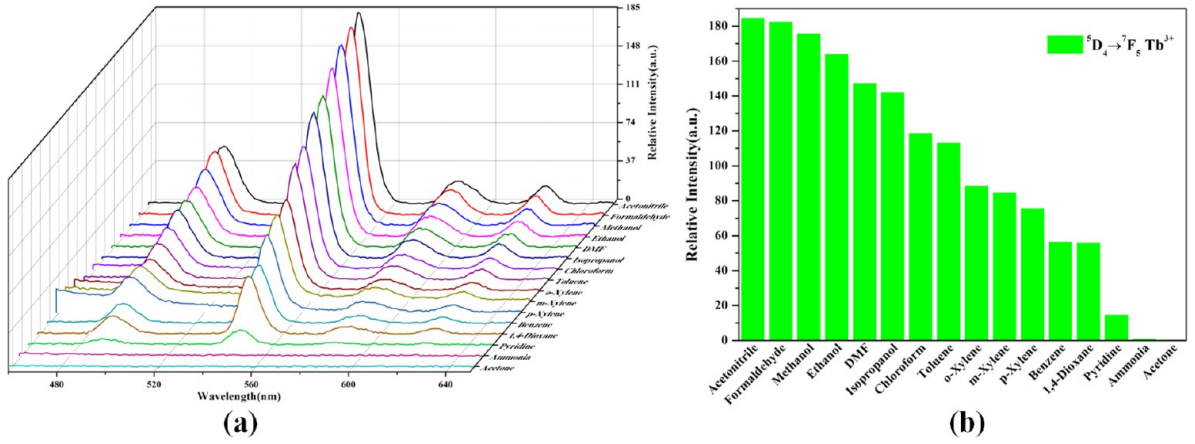

Figure 7. (a) PL spectra and (b) the $^5D_4 \rightarrow {}^7F_5$ transition intensities of **2** dispersed into different solvents when excited at 300 nm.

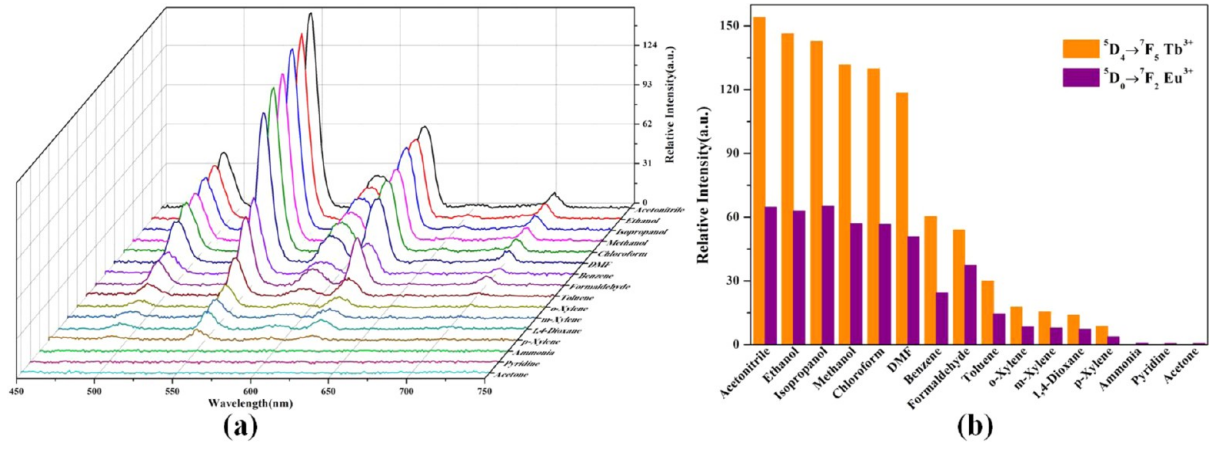

Figure 8. (a) PL spectra and (b) the $^5D_0 \rightarrow {}^7F_2$ and $^5D_4 \rightarrow {}^7F_5$ transition intensities of **1a** dispersed into different solvents when excited at 300 nm.

These Ln-MOFs are stable and insoluble in aqueous sodium halide solution, confirmed by the PXRD (Supporting Information Figure S7). Different kinds of halogenic anions of F^- (NaF), Cl^- (NaCl), Br^- (NaBr), and I^- (NaI) have been introduced to the system of Ln-MOFs **1**, **2**, and **1a**. Compared with **1**, **2**, and **1a** in H_2O, the emission intensities in NaF aqueous solution almost reduce to zero, while the emission intensities in NaCl, NaBr, and NaI basically have no change (Supporting Information Figures S8−S10). Therefore, F^- (NaF) anion can be considered as recognizable anion to study its quenching effect on the fluorescent intensity in suspension. The emission spectra of **1**, **2**, and **1a** in suspension-state at room temperature are shown in Figure 5. By comparison with their luminescent spectra in solid state, the emission bands have no shift and only the emission intensity turns weaker in H_2O excited at 300 nm. Considering that the maximum emission intensities of Eu^{3+} and Tb^{3+} in **1a** are comparatively close, **1a** of the doped samples is selected as a reference sample to conduct the following research. **1a** also exhibits an obvious response with increasing the content of F^-

dx.doi.org/10.1021/ic400770j | Inorg. Chem. 2013, 52, 8082−8090

anion. Interestingly, the emission intensity of Tb^{3+} decrease slower than Eu^{3+}, although the intensity of Eu^{3+} and Tb^{3+} simultaneously decrease once NaF is added to **1a**. It is clearly found that when a 3 equiv portion of F^- has been introduced to the system of **1a**, the maximum emission intensity of Tb^{3+} at 544 nm is stronger than Eu^{3+} at 614 nm, while the emission intensity of Tb^{3+} is initially weaker than Eu^{3+} (Figure 5c).

To further examine the potential of **1**, **2**, and **1a** for the sensing of organic small molecules, their luminescent recognition and selectivity in different solvent suspensions were investigated. Before the solvent-suspension luminescent measurements, the stability and insolubility of the frameworks in common organic solvents, such as methanol, ethanol, isopropanol, acetonitrile, 1,4-dioxane, acetone, benzene, toluene, *o*-xylene, *m*-xylene, *p*-xylene, formaldehyde (∼ 40% formaldehyde solution), ammonia, chloroform, and pyridine were confirmed by PXRD (Supporting Information Figure S14). As shown in Figures 6–8, their PL spectra are largely dependent on the solvents, particularly in the case of formaldehyde and acetone for **1** and acetonitrile and acetone for **2** and **1a**, which exhibit the most noticeable enhancing and quenching effects, respectively. Such solvent-dependent luminescent properties are of interest for the sensing of formaldehyde, acetonitrile, and acetone solvent molecules, which are very harmful to human beings, especially formaldehyde as one of the most important pollutants from interior decoration. Therefore, the effects of formaldehyde, acetonitrile, and acetone on the luminescent intensities of these compounds have been examined in more detail.

Ln-MOFs **1**, **2**, and **1a** were dispersed into 1,4-dioxane, toluene, and formaldehyde, respectively, as the standard suspensions, while the content of formaldehyde/acetone for **1** (acetonitrile/acetone for **2** and **1a**) was gradually increased to monitor the emissive intensities. It was noticeable that the luminescent intensity of the suspension of **1** increased with the addition of formaldehyde, as shown in Figure 9**a**, and the enhancement was nearly proportional to the concentration of formaldehyde. Similarly, with the introduction of acetonitrile into the standard suspensions of **2** and **1a**, their luminescent intensities were proportionally enhanced by the concentration of acetonitrile (Figures 10a and 11a). On the other hand, adding acetone into the standard suspensions of **1**, **2**, and **1a** resulted in an obvious decrease of their luminescent intensities, which almost disappeared at an acetone content of 9.09, 8.26, and 11.11 vol % for **1**, **2**, and **1a**, respectively (Figures 9b, 10b, and 11b). The decreasing trend of the largest luminescent intensities versus the volume ratio of acetone could be well fitted with a first-order exponential decay (Supporting Information Figures S15–S17), indicating that luminescent quenching of **1**, **2**, and **1a** by acetone is diffusion-controlled.[20] The above results indicate that Ln-MOFs **1**, **2**, and **1a** are promising chemical sensors for small molecule pollutants.

The radii of F^- is 1.19 Å, smaller than Cl^- (1.67 Å), Br^- (1.82 Å), and I^- (2.06 Å).[21] Hence, the F^- can be more easily trapped in the cavities of the MOF than other halogen anions and thus result in the quenching effect on the luminescent emission. Considering the van der Waals radius, the organic molecules could be trapped on the surface of the MOF to influence the energy transfer from the ligand to the lanthanide center, and consequently results in luminescent enhancement or quenching. These phenomena were previously observed in Eu or Tb-MOFs with luminescent response.[4m,19] It is very exciting that such Ln-MOFs can display highly selective

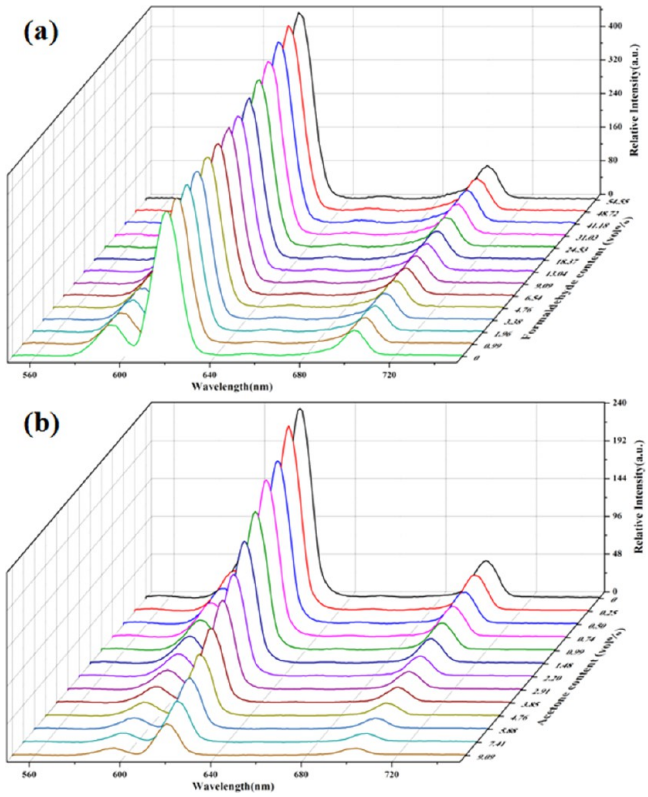

Figure 9. PL spectra of **1**/1,4-dioxane suspension in the presence of various amounts of (a) formaldehyde and (b) acetone solvent, respectively (excited at 300 nm).

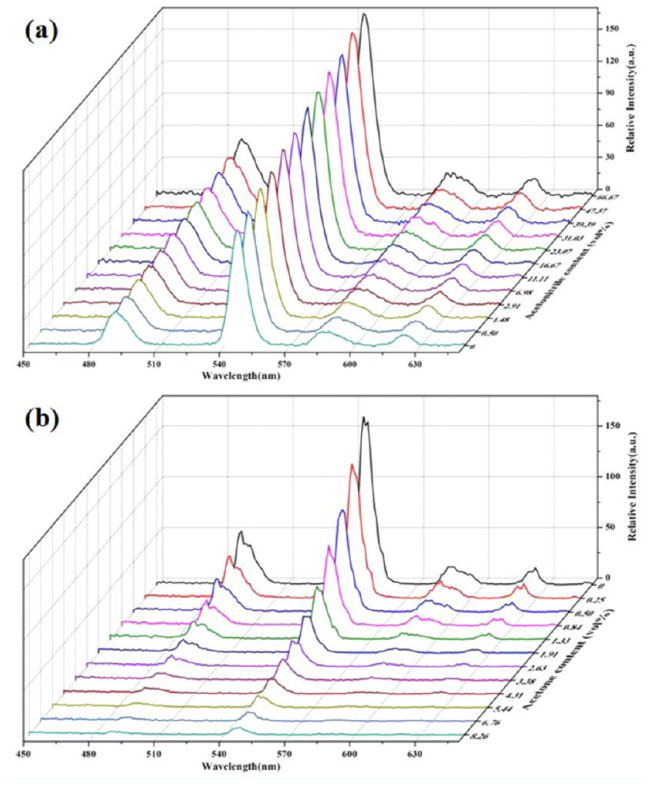

Figure 10. PL spectra of **2**/toluene suspension in the presence of various amounts of (a) acetonitrile and (b) acetone solvent, respectively (excited at 300 nm).

dx.doi.org/10.1021/ic400770j | *Inorg. Chem.* 2013, 52, 8082–8090

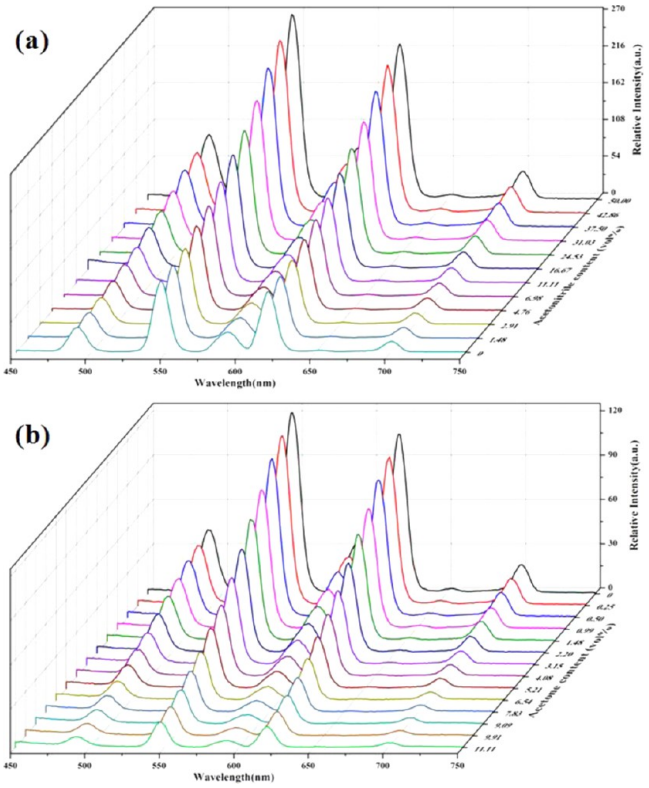

Figure 11. PL spectra of **1a**/formaldehyde suspension in the presence of various amounts of (a) acetonitrile and (b) acetone solvent, respectively (excited at 300 nm).

luminescent response in the visible-light range, so that the environmental pollutants could be expected to be directly detected by the eye.

CONCLUSIONS

In summary, we have successfully synthesized a series of novel multifunctional Ln-MOFs based on mixed ligand approach via hydrothermal reactions. The frameworks are isostructurally constructed by dinuclear Ln_2 units, to possess **tfz-d** topology with the short (Schläfli) vertex symbol $\{4^3\}_2\{4^6{\cdot}6^{18}{\cdot}8^4\}$.The studies of luminescent properties show the typical luminescence of Eu^{3+} (**1**), Tb^{3+} (**2**), and Eu^{3+}/Tb^{3+} (**1a**−**e**) in the visible region. Ln-MOFs **1**, **2**, and **1a** display high-sensitivity luminescent sensing functions to fluoride anion and small-molecules, particularly formaldehyde, acetonitrile, and acetone. This work points out that these Ln-MOFs and their doped samples are expected to play an important role in the applications such as luminescent probe for the recognition of anions and poisonous small molecule solvents.

ASSOCIATED CONTENT

Supporting Information

The FTIR spectra (Figure S1), the channel of the Ln-MOFs (Figure S2), the schematic diagram of hydrogen bonds (Figure S3), PXRD patterns (Figures S4, S7, S14), TGA (Figure S5), PL spectra (Figures S6, S8−S13), fluorescence data fitting (Figures S15−S17), ICP results (Table S1), Lanthanide geometry analysis by using the Shape software (Table S3), selected bond lengths and angles (Table S3), and X-ray crystallographic files (CIF) for **1** and **2**. This material is available free of charge via the Internet at http://pubs.acs.org.

AUTHOR INFORMATION

Corresponding Author

*E-mail: shiwei@nankai.edu.cn (W.S.); pcheng@nankai.edu.cn (P.C.). Fax: (+86)22-23502458.

Notes

The authors declare no competing financial interest.

ACKNOWLEDGMENTS

We gratefully acknowledge the "973" program (2012CB821702), NSFC (21171100 21151001 and 90922032), and 111 Project (B12015).

REFERENCES

(1) (a) Maspoch, D.; Ruiz-Molina, D.; Veciana, J. *Chem. Soc. Rev.* **2007**, *36*, 770. (b) Allendorf, M. D.; Bauer, C. A.; Bhakta, R. K.; Houk, R. J. T. *Chem. Soc. Rev.* **2009**, *38*, 1330. (c) Kuppler, R. J.; Timmons, D. J.; Fang, Q. R.; Li, J. R.; Makal, T. A.; Young, M. D.; Yuan, D. Q.; Zhao, D.; Zhuang, W. J.; Zhou, H. C. *Coord. Chem. Rev.* **2009**, *253*, 3042. (d) Kreno, L. E.; Leong, K.; Farha, O. K.; Allendorf, M.; Van Duyne, R. P.; Hupp, J. T. *Chem. Rev.* **2012**, *112*, 1105.

(2) (a) Wang, C.; Zhang, T.; Lin, W.-B. *Chem. Rev.* **2012**, *112*, 1084. (b) Cui, Y.; Yue, Y.; Qian, G.; Chen, B. *Chem. Rev.* **2012**, *112*, 1126. (c) Meek, S. T.; Greathouse, J. A.; Allendorf, M. D. *Adv. Mater.* **2011**, *23*, 249. (d) Wu, P.; Wang, J.; Li, Y.; He, C.; Xie, Z.; Duan, C. *Adv. Funct. Mater.* **2011**, *21*, 2788. (e) Chen, B.; Wang, L.; Zapata, F.; Qian, G.; Lobkovsky, E. B. *J. Am. Chem. Soc.* **2008**, *130*, 6718.

(3) (a) Zhang, Z.-H.; Song, Y.; Okamura, T.; Hasegawa, Y.; Sun, W.-Y.; Ueyama, N. *Inorg. Chem.* **2006**, *45*, 2896. (b) Wong, K.-L.; Law, G.-L.; Yang, Y.-Y.; Wong, W.-T. *Adv. Mater.* **2006**, *18*, 1051. (c) Li, Z.-Y.; Zhu, G.-S.; Guo, X.-D.; Zhao, X.-J.; Jin, Z.; Qiu, S.-L. *Inorg. Chem.* **2007**, *46*, 5174. (d) Harbuzaru, B. V.; Corma, A.; Rey, F.; Atienzar, P.; Jordá, J. L.; García, H.; Ananias, D.; Carlos, L. D.; Rocha, J. *Angew. Chem., Int. Ed.* **2008**, *47*, 1080. (e) Chen, B.; Wang, L.; Xiao, Y.; Fronczek, F. R.; Xue, M.; Cui, Y.; Qian, G. *Angew. Chem., Int. Ed.* **2009**, *48*, 500. (f) Zhang, X.; Ballem, M. A.; Hu, Z.-J.; Bergman, P.; Uvdal, K. *Angew. Chem., Int. Ed.* **2011**, *50*, 5729.

(4) (a) Lan, A. J.; Li, K. H.; Wu, H. H.; Olson, D. H.; Emge, T. J.; Ki, W.; Hong, M. C.; Li, J. *Angew. Chem., Int. Ed.* **2009**, *48*, 2334. (b) Xiao, Y. Q.; Cui, Y. J.; Zheng, Q.; Xiang, S. C.; Qian, G. D.; Chen, B. L. *Chem. Commun.* **2010**, *46*, 5503. (c) Zhang, J. Z.; Xiang, S. C.; Rao, X. T.; Zheng, Q.; Fronczek, F. R.; Qian, G. D.; Chen, B. L. *Chem. Commun.* **2010**, *46*, 7205. (d) Guo, Z. Y.; Xu, H.; Su, S. Q.; Cai, J. F.; Dang, S.; Xiang, S. C.; Qian, G. D.; Zhang, H. J.; O'Keeffed, M.; Chen, B. L. *Chem. Commun.* **2011**, *47*, 5551. (e) Jayaramulu, K.; Narayanan, R. P.; George, S. J.; Maji, T. K. *Inorg. Chem.* **2012**, *51*, 10089. (f) Wu, P.; Wang, J.; He, C.; Zhang, X.; Wang, Y.; Liu, T.; Duan, C. *Adv. Funct. Mater.* **2012**, *22*, 1698. (g) Li, Y.; Zhang, S. S.; Song, D. T. *Angew. Chem., Int. Ed.* **2013**, *125*, 738. (h) Tang, Q.; Liu, S. X.; Liu, Y. W.; Miao, J.; Li, S. J.; Zhang, L.; Shi, Z.; Zheng, Z. P. *Inorg. Chem.* **2013**, *52*, 2799. (i) Sun, C.-Y.; Wang, X.-L.; Qin, C.; Jin, J.-L.; Su, Z.-M.; Huang, P.; Shao, K.-Z. *Chem.—Eur. J.* **2013**, *19*, 3639. (j) Wang, J.-H.; Li, M.; Li, D. *Chem. Sci.* **2013**, *4*, 1793. (k) Liu, G.; Qin, Y.; Jing, L.; Wei, G.; Li, H. *Chem. Commun.* **2013**, *49*, 1699. (l) Hou, S.; Liu, Q.-K.; Ma, J.-P.; Dong, Y.-B. *Inorg. Chem.* **2013**, *52*, 3225. (m) Li, H.; Shi, W.; Zhao, K.; Niu, Z.; Li, H.; Cheng, P. *Chem.—Eur. J.* **2013**, *19*, 3358. (n) Chen, Y.; Ma, S.-Q. *Rev. Inorg. Chem.* **2012**, *32*, 81.

(5) (a) Richardson, F. S. *Chem. Rev.* **1982**, *82*, 541. (b) Parker, D.; Williams, J. A. G. *J. Chem. Soc., Dalton Trans.* **1996**, 3613. (c) Ma, L.; Evans, O. R.; Foxman, B. M.; Lin, W. B. *Inorg. Chem.* **1999**, *38*, 5837. (d) Sá de, G. F.; Malta, O. L.; Donegá de, M. C.; Simas, A. M.; Longo, R. L.; Santa-Cruz, P. A.; Silva Jr da, E. F. *Coord. Chem. Rev.* **2000**, *196*, 165.

(6) (a) Yamase, T.; Naruke, H. *J. Phys. Chem. B* **1999**, *103*, 8850. (b) de Lill, D. T.; de Bettencourt-Dias, A.; Cahill, C. L. *Inorg. Chem.* **2007**, *46*, 3960. (c) Evans, R. C.; Carlos, L. D.; Douglas, P.; Rocha, J. *J. Mater. Chem.* **2008**, *18*, 1100. (d) He, G.; Guo, D.; He, C.; Zhang, X.; Zhao, X.; Duan, C. *Angew. Chem., Int. Ed.* **2009**, *48*, 6132. (e) Biju, S.;

Ambili Raj, D. B.; Reddy, M. L. P.; Jayasankar, C. K.; Cowley, A. H.; Findlater, M. *J. Mater. Chem.* **2009**, *19*, 1425. (f) Guo, H.; Zhu, Y.; Qiu, S.; Lercher, J. A.; Zhang, H. *Adv. Mater.* **2010**, *22*, 4190. (g) Li, G.; Hou, Z.; Peng, C.; Wang, W.; Cheng, Z.; Li, C.; Lian, H.; Lin, J. *Adv. Funct. Mater.* **2010**, *20*, 3446. (h) Luo, F.; Batten, S. R. *Dalton Trans.* **2010**, *39*, 4485. (i) Choi, C.-L.; Yen, Y.-F.; Sung, H. H. Y.; Siu, A. W. H.; Jayarathne, S. T.; Wong, K. S.; Williams, I. D. *J. Mater. Chem.* **2011**, *21*, 8547. (j) Cui, Y.; Xu, H.; Yue, Y.; Guo, Z.; Yu, J.; Chen, Z.; Gao, J.; Yang, Y.; Qian, G.; Chen, B. *J. Am. Chem. Soc.* **2012**, *134*, 3979.

(7) (a) Wang, P.; Ma, J.-P.; Dong, Y.-B.; Huang, R.-Q. *J. Am. Chem. Soc.* **2007**, *129*, 10620. (b) White, K. A.; Chengelis, D. A.; Gogick, K. A.; Stehman, J.; Rosi, N. L.; Petoud, S. *J. Am. Chem. Soc.* **2009**, *131*, 18069. (c) Wang, P.; Ma, J.-P.; Dong, Y.-B. *Chem.—Eur. J.* **2009**, *15*, 10432. (d) Liu, K.; You, H.; Zheng, Y.; Jia, G.; Song, Y.; Huang, Y.; Yang, M.; Jia, J.; Guo, N.; Zhang, H. *J. Mater. Chem.* **2010**, *20*, 3272. (e) Lan, Y.-Q.; Jiang, H.-L.; Li, S.-L.; Xu, Q. *Adv. Mater.* **2011**, *23*, 5015. (f) Chen, C.-X.; Liu, Q.-K.; Ma, J.-P.; Dong, Y.-B. *J. Mater. Chem.* **2012**, *22*, 9027.

(8) (a) Piguet, C.; Bünzli, J.-C. G. *J. Am. Chem. Soc.* **1993**, *115*, 8197. (b) Elhabiri, M.; Scopelliti, R.; Bünzli, J.-C. G.; Piguet, C. *J. Am. Chem. Soc.* **1999**, *121*, 10747. (c) Deiters, E.; Gumy, F.; Bünzli, J.-C. G. *Eur. J. Inorg. Chem.* **2010**, 2723. (d) Allali, M.; Mulatier, J.-C.; Guennic, B. L.; Zwier, J. M.; Baldeck, P. L.; Bünzli, J.-C. G.; Andraud, C.; Lamarque, L.; Maury, O. *Inorg. Chem.* **2011**, *50*, 4987. (e) Sorgho, L. A.; Nozary, H.; Aebischer, A.; Bünzli, J.-C. G. *J. Am. Chem. Soc.* **2012**, *134*, 12675. (f) Arakcheeva, A.; Logvinovich, D.; Chapuis, G.; Morozov, V.; Eliseeva, S. V.; Bünzli, J.-C. G.; Pattisonaf, P. *Chem. Sci.* **2012**, *3*, 384.

(9) (a) Torelli, S.; Imbert, D.; Cantuel, M.; Bernardinelli, G.; Delahaye, S.; Hauser, A.; Bünzli, J.-C. G.; Piguet, C. *Chem.—Eur. J.* **2005**, *11*, 3228. (b) Dalla-Favera, N.; Hamacek, J.; Borkovec, M.; Jeannerat, D.; Ercolani, G.; Piguet, C. *Inorg. Chem.* **2007**, *46*, 9312. (c) Canard, G.; Koeller, S.; Bernardinelli, G.; Piguet, C. *J. Am. Chem. Soc.* **2008**, *130*, 1025. (d) Favera, N.; Guénée, L.; Bernardinelli, G.; Piguet, C. *Dalton. Trans.* **2009**, 7625. (f) Aboshyan-Sorgho, L.; Besnard, C.; Pattison, P.; Kittilstved, K. R.; Aebischer, A.; Bünzli, J.-C. G.; Hauser, A.; Piguet, C. *Angew. Chem., Int. Ed.* **2011**, *50*, 4108. (g) Zaïm, A.; Favera, N. D.; Guénée, L.; Nozary, H.; Hoang, T. N. Y.; Eliseeva, S. V.; Petoudc, S.; Piguet, C. *Chem. Sci.* **2013**, *4*, 1125.

(10) (a) Zhao, B.; Gao, H. L.; Chen, X. Y.; Cheng, P.; Shi, W.; Liao, D. Z.; Yan, S. P.; Jiang, Z.-H. *Chem.—Eur. J.* **2006**, *12*, 149. (b) Zhao, B.; Chen, X. Y.; Chen, Z.; Shi, W.; Cheng, P.; Yan, S. P.; Liao, D. Z. *Chem. Commun.* **2009**, 3113. (c) Xia, J.; Zhao, B.; Wang, H. S.; Shi, W.; Ma, Y.; Song, H. B.; Cheng, P.; Liao, D. Z.; Yan, S. P. *Inorg. Chem.* **2007**, *46*, 3450. (d) Zhao, X. Q.; Zhao, B.; Ma, Y.; Shi, W.; Cheng, P.; Jiang, Z. H.; Liao, D. Z.; Yan, S. P. *Inorg. Chem.* **2007**, *46*, 5832. (e) Zhao, X. Q.; Zhao, B.; Shi, W.; Cheng, P. *Inorg. Chem.* **2009**, *48*, 11048. (f) Zhao, X. Q.; Zhao, B.; Shi, W.; Cheng, P.; Liao, D. Z.; Yan, S. P. *Dalton Trans.* **2009**, 2281.

(11) (a) Kanungo, B. K.; Baral, M.; Bhattacharya, S.; Sahoo, Y. *Synth. Commun.* **2003**, *33*, 3159. (b) Cheng, Y. J. *Friend Chem. Ind.* **2006**, *12*, 41. (c) Liu, Z. P.; Wang, X. T. *Chin. Rare Earths* **2004**, *25*, 39.

(12) (a) Sheldrick, G. M. *Acta Crystallogr.* **2008**, *A64*, 112. (b) Dolomanov, O. V.; Bourhis, L. J.; Gildea, R. J.; Howard, J. A. K.; Puschmann, H. *J. Appl. Crystallogr.* **2009**, *42*, 339.

(13) (a) Muetterties, E. L.; Guggenberger, L. J. *J. Am. Chem. Soc.* **1974**, *96*, 1748. (b) Drew, M. G. B. *Coord. Chem. Rev.* **1977**, *24*, 179. (c) Zabrodsky, H.; Peleg, S.; Avnir, D. *J. Am. Chem. Soc.* **1992**, *114*, 7843. (d) Pinsky, M.; Avnir, D. *Inorg. Chem.* **1998**, *37*, 5575.

(14) (a) Blatov, V. A. *IUCr Comp. Commun. Newslett.* **2006**, *7*, 4 ; available at http://iucrcomputing.ccp14.ac.uk/iucr-top/comm/ccom/newsletters/2006nov/. (b) Blatov, V. A. http://www.topos.ssu.samara.ru/starting.html. (c) O'Keeffe, M. *Reticular Chemistry Structure Resource*. http://rcsr.anu.edu.au/.

(15) (a) Yan, Li.; Yue, Q.; Jia, Q.-X.; Lemercier, G.; Gao, E.-Q. *Cryst. Growth Des.* **2009**, *9*, 2984. (b) Yang, Q.-Y.; Li, K.; Luo, J.; Pan, M.; Su, C.-Y. *Chem. Commun.* **2011**, *47*, 4234.

(16) (a) Garibay, S. J.; Stork, J. R.; Wang, Z. Q.; Cohen, S. M.; Telfer, S. G. *Chem. Commun.* **2007**, 4881. (b) Luo, F.; Che, Y.; Zheng, J. *Cryst. Growth Des.* **2008**, *8*, 2006. (c) Liu, G.-X.; Huang, Y.-Q.; Chu, Q.; Okamura, T.; Sun, W.-Y.; Liang, H.; Ueyama, N. *Cryst. Growth Des.* **2008**, *8*, 3233. (d) Davies, R. P.; Less, R. J.; Lickiss, P. D.; Robertson, K.; White, A. J. P. *Inorg. Chem.* **2008**, *47*, 9958. (e) Xu, G. J.; Zhao, Y. H.; Shao, K. Z.; Lan, Y. Q.; Wang, X. L.; Su, Z. M.; Yan, L. K. *CrystEngComm.* **2009**, *11*, 1842. (g) Li, H.-H.; Shi, W.; Xu, N.; Zhang, Z.-J.; Niu, Z.; Han, T.; Cheng, P. *Cryst. Growth Des.* **2012**, *12*, 2602.

(17) (a) Vicentini, G.; Zinner, L. B.; Zukerman-Schpector, J.; Zinner, K. *Coord. Chem. Rev.* **2000**, *196*, 353. (b) Wang, X. J.; Cen, Z. M.; Ni, Q. L.; Jiang, X. F.; Lian, H. C.; Gui, L. C.; Zuo, H. H.; Wang, Z. Y. *Cryst. Growth Des.* **2010**, *10*, 2960. (c) Lin, Z. J.; Xu, B.; Liu, T. F.; Cao, M. N.; Lü, J.; Cao, R. *Eur. J. Inorg. Chem.* **2010**, 3842. (d) Peng, G.; Qiu, Y. C.; Liu, Z. H.; Liu, B.; Deng, H. *Cryst. Growth Des.* **2010**, *10*, 114.

(18) (a) Tedeschi, C.; Azema, J.; Gornitzka, H.; Tisnes, P.; Picard, C. *Dalton Trans.* **2003**, 1738. (b) Dias, A. B.; Viswanathan, S. *Chem. Commun.* **2004**, 1024. (c) Sun, Y.-Q.; Zhang, J.; Chen, Y.-M.; Yang, G.-Y. *Angew. Chem., Int. Ed.* **2005**, *44*, 5814.

(19) Arnaud, N.; Vaquer, E.; Georges, J. *Analyst* **1998**, *123*, 261.

(20) Chen, B.; Yang, Y.; Zapata, F.; Lin, G.; Qian, G.; Lobkovsky, E. B. *Adv. Mater.* **2007**, *19*, 1693.

(21) Miessler, G. L.; Tarr, D. A. *Inorganic Chemistry, International Edition*, 3rd ed.; Prentice Hall, Upper Saddle River, NJ, 2004; Appendix B, pp 669−670.